Immunobiology 225 (2020) 151860

Contents lists available at ScienceDirect

Immunobiology

journal homepage: www.elsevier.com/locate/imbio

A combination of check-point blockade and α-galactosylceramide elicits long-lasting suppressive effects on murine hepatoma cell growth in vivo

Kazuhito Ishii, Masumi Shimizu, Hideki Kogo, Yasuyuki Negishi, Hideto Tamura, Rimpei Morita, Hidemi Takahashi*

Department of Microbiology and Immunology, Nippon Medical School, 1-1-5 Sendagi, Bunkyo-ku, Tokyo, 113-8602, Japan

ARTICLE INFO

Keywords:
anti-PD-1 monoclonal antibody (mAb)
CTLs
DCs
CD1d
α-galactosylceramide (α-GalCer)

ABSTRACT

Immunotherapy for cancer cells induced by interfering with PD-1/PD-L1 engagement via check-point blockades was initiated by tumour-specific PD-1$^+$ CD8$^+$ cytotoxic T lymphocytes (CTLs) within a tumour mass and eliminate the tumour. Here, we used C57BL/6 (B6) mice implanted with the syngeneic hepatoma cell line Hepa1-6-1, and confirmed that the dendritic cells (DCs) within Hepa1-6-1 tumour mass were tolerogenic with downmodulated co-stimulatory molecules by tumour-derived factors. Although Hepa1-6-1 cells did not prime tumour-specific CTLs within the tumour, specific CTLs primed in the regional lymph nodes seemed to be invaded into the tumour mass. The specific CTLs gained PD-1$^+$ expression when associated with PD-L1$^+$ Hepa1-6-1 cells within the tumour mass. Their cytotoxic activity in vivo was revitalised after intraperitoneal (i.p.) administration of the anti-PD-1 monoclonal antibody (mAb), indicating that PD-1/PD-L1 engagement within the tumour was abrogated by check-point blockade. Nonetheless, the tolerogenic DCs within the Hepa1-6-1 tumour mass remained tolerogenic even after three shots of PD-1-blockade administration, and the suppressed Hepa1-6-1 growth was revisited. In this study, we show here an excellent therapeutic effect consisting of three injections of anti-PD1 mAb and the sequential administration of the CD1d molecule-restricted ligand α-galactosylceramide (α-GalCer), an immuno-potent lipid/glycolipid, which converts tolerogenic DCs into immunogenic DCs with upregulated expression of co-stimulatory molecules. The α-GalCer-activated DCs secreted a large amount of IL-12, which can activate tumour-specific CTLs in vivo. The check-point blockade was not sufficiently effective, but the dose needed for tumour eradication was reduced by 90% when tumour-bearing mice were also administered i.p. α-GalCer.

1. Introduction

Tumour cells and tumour-specific CD8$^+$ cytotoxic T cells (CTLs) primarily function in a situation of mutual suppression through tethering engagement with PD-1/PD-L1 within the tumour mass (Benson et al., 2010; Blank et al., 2005; Prosser et al., 2012). When the mutual suppression is abrogated by either anti-PD-1- or anti-PD-L1-specific monoclonal antibodies (mAbs), CD8$^+$ CTLs are released by disconnecting the tethering chains, thus regaining their cytotoxicity. These activated CD8$^+$ CTLs will attack and eliminate tumour cells. Therefore, CD8$^+$ CTLs should be induced to infiltrate into tumours before examining the effect of check-point blockade treatment. However, the tumour mass is typically surrounded by tolerogenic dendritic cells (DCs) (Harimoto et al., 2013) induced by soluble tumour cell-derived factors (Harimoto et al., 2013; Kozako et al., 2011; Matsuhashi et al., 2014). These tolerogenic DCs do not help induce tumour-specific CD8$^+$ cells but instead inhibit induction of CTLs from naïve T cells.

The precise mechanisms by which tumour-specific CD8$^+$ CTLs are established and are able to invade tumours are unknown. We have observed that CD8$^+$ CTLs can be induced from naïve T cells by immunogenic DCs that have captured tumour-derived antigens and cross-reactively present the tumour epitope(s) in association with class I MHC and appropriate co-stimulatory molecules (McDonnell et al., 2010; Nizzoli et al., 2016). Nevertheless, immunogenic DCs cannot typically be found within a growing tumour mass. This lack may occur because tolerogenic DCs are predominantly induced to reside in the growing

Abbreviations: α-GalCer, α-galactosylceramide; CCM, complete culture medium; CTLs, cytotoxic T lymphocytes; DCs, dendritic cells; i.p., intraperitoneal; mAb, monoclonal antibody; s.c., subcutaneous

* Corresponding author.
E-mail addresses: kxi@nms.ac.jp (K. Ishii), kita-g@nms.ac.jp (M. Shimizu), s8037@nms.ac.jp (H. Kogo), negi@nms.ac.jp (Y. Negishi), tam@nms.ac.jp (H. Tamura), morita@nms.ac.jp (R. Morita), htkuhkai@nms.ac.jp (H. Takahashi).

https://doi.org/10.1016/j.imbio.2019.10.009
Received 8 May 2019; Received in revised form 28 October 2019; Accepted 29 October 2019
Available online 04 November 2019

tumours by tumour-derived factors, such as transforming growth factor (TGF)-beta1, vascular endothelial growth factor (VEGF) and alpha-fetoprotein (AFP) (Harimoto et al., 2013); thus, functional tumour-specific $CD8^+$ CTLs cannot be elicited from naïve T cells within the growing tumour mass. Only immunogenic DCs expressing a sufficient magnitude of co-stimulatory molecules, such as CD80, CD86 and CD40, can promote differentiation of naïve T cells into functional $CD8^+$ CTLs (Kumari et al., 2013).

In our previous study (Harimoto et al., 2013), we established two distinct hepatoma cell lines (Hepa1-6-1 and Hepa1-6-2 cells) from the known hepatoma cell line Hepa1-6 (H-2^b) (Ishii et al., 2004; Nakatsuka et al., 1999). After subcutaneous implantation into syngeneic C57BL/6 (B6) mice (H-2^b), the Hepa1-6-1 cells formed a solid tumour mass. We thoroughly examined the Hepa1-6-2 cells and confirmed that their regression was induced through specific cytotoxicity mediated by $CD8^+$ CTLs within the Hepa1-6-2 tumour mass. The $CD8^+$ CTLs obtained from the Hepa1-6-2 tumour mass were confirmed to have the ability to eliminate both Hepa1-6-1 and Hepa1-6-2 cells nearly equally (Harimoto, et al., 2013).

Moreover, we investigated B6 mice simultaneously transplanted with Hepa1-6-1 cells in the left and Hepa1-6-2 cells in the right abdominal regions. The Hepa1-6-1 cells were seemingly unaffected by the specific $CD8^+$ CTLs elicited in the Hepa1-6-2 tumour mass, and the Hepa1-6-1 mass seemed to actively grow beside the Hepa1-6-2 tumour mass (Harimoto et al., 2013). Nonetheless, here, we confirmed the existence of PD-1-expressing $CD8^+$ CTLs within the PD-L1-expressing Hepa1-6-1 tumour mass. Unexpectedly, when various doses of anti-PD-1 mAb were administered to these mice via intraperitoneal (i.p.) injection, the growth of the Hepa1-6-1 mass stopped, and the tumour size was reduced in a dose-dependent manner. This effect could have occurred because Hepa1-6-2-specific $CD8^+$ CTLs intruded into the Hepa1-6-1 tumour mass, and the cytotoxicity of the Hepa1-6-2-specific $CD8^+$ CTLs was suppressed by mutual engagement between PD-1 on the Hepa1-6-2-specific $CD8^+$ CTLs and PD-L1 on the Hepa1-6-1 cells, as established in vivo. Additionally, check-point blockade may sever the tethering chain to activate CTL cytotoxicity in vivo.

Furthermore, we found regression of Hepa1-6-1 cell growth in the absence of the Hepa1-6-2 tumour mass after check-point blockade administration. Indeed, we confirmed that PD-1-expressing Hepa1-6-1-specific $CD8^+$ CTLs are present within the Hepa1-6-1 tumour mass, although such CTLs are not induced within the tumour mass because tolerogenic DCs elicited by tumour-derived factors reside there. This regression may be due to elicitation of Hepa1-6-1-specific $CD8^+$ CTLs in other locations, such as regional lymph nodes, by immunogenic DCs expressing tumour-derived epitope(s) associated with class I MHC augmented by co-stimulatory molecules that have invaded into the tumour mass. In such cases, i.p. administration of anti-PD-1 mAb induces apparent inhibition of Hepa1-6-1 tumour growth in vivo. Overall, when Hepa1-6-1-specific $CD8^+$ CTLs are elicited outside of the tumour mass, PD-1^+ CTLs may intrude into the PD-L1-expressing tumour mass, and the PD-1/PD-L1 engagement established in vivo can be abrogated by i.p. administration of PD-1-blocking antibody.

However, three PD-1-blockade i.p. injections will not convert tolerogenic DCs to an immunogenic state with enhanced co-stimulatory molecule expression, and a long-lasting effect requires a number of additional injections or the administration of a higher dose of the anti-PD-1 mAb that is likely toxic. Finally, Hepa1-6-1 mass growth recurred in our mouse system, indicating that we should consider another therapy to control tumour growth. To overcome the limitation of the effects of PD-1 blockade in this mouse model, here, on the basis of our recent findings (Kogo et al., 2017), we show the effectiveness of combination therapy with three PD-1-blockade injections and the sequential administration of the CD1d molecule-restricted ligand α-galactosylceramide (α-GalCer) (Funakoshi Co., Ltd., Tokyo, Japan), which is an immuno-potent lipid/glycolipid that converts tolerogenic DCs into an immunogenic state (Ichikawa et al., 2016; Kogo et al., 2017; Murakami et al., 2015; Otsuka et al., 2018). This combination therapeutic approach exhibited stable and profound effects on tumour regression.

2. Materials and methods

2.1. Mice

Six-week-old female B6 mice and $CD1d^{-/-}$ mice on a B6 background were purchased from Charles River Japan (Kanagawa, Japan) and the Jackson Laboratory (Bar Harbor, ME), respectively. The mice were maintained in microisolator cages under pathogen-free conditions and were used between 7 and 9 weeks of age. We conducted all animal experiments according to the Guide for the Care and Use of Laboratory Animals by the National Institutes of Health (NIH, Bethesda, MD). All animal experiments were approved by the Review Board of Nippon Medical School (Tokyo, Japan).

2.2. Cell culture and tumour cell line

The Hepa1-6-1 cell line was established from the murine hepatoma Hepa1-6 cells (H-2^b), which were purchased from the American Type Culture Collection (ATCC, VA) as described previously (Kogo et al., 2017). In brief, Hepa1-6-1 cells were harvested from cells purified from a surgically removed tumour mass that grew for 3 months after the subcutaneous (s.c.) implantation of Hepa1-6 cells into syngeneic B6 mice. The Hepa1-6-1 cells were cultured at 37 °C with 8% CO_2 in Dulbecco's modified Eagle's medium (DMEM) containing 4.5 g/l of D-glucose (Thermo Fisher Scientific, Waltham, MA), 10 mM HEPES (Thermo Fisher Scientific), 50 units/ml of penicillin (Thermo Fisher Scientific), 50 μg/ml of streptomycin (Thermo Fisher Scientific) and 10% heat-inactivated foetal calf serum (FCS; Thermo Fisher Scientific). Yac-1 cells were also purchased from ATCC. Yac-1 and immunocompetent cells, such as CTLs and DCs, were cultured at 37 °C with 5% CO_2 in RPMI 1640-based complete culture medium (CCM) (Takahashi et al., 1996) containing 0.025 mM 2-mercaptoethanol, 1 mM L-glutamine, 0.5 mM sodium pyruvate, 0.05 mM non-essential amino acids, a mixture of vitamins, 5 mM HEPES, 25 units/ml penicillin, 25 μg/ml streptomycin, and 10% heat-inactivated FCS.

2.3. Implantation of Hepa1-6-1 cells in B6 mice and $CD1d^{-/-}$ mice

Syngeneic B6, and $CD1d^{-/-}$ mice were implanted s.c. with 1×10^7 Hepa1-6-1 cells in the abdominal region. For estimation of tumour mass volume, the major axis (a) and the minor axis (b) were monitored every other day with a calliper, and the tumour volume (V) was calculated using the formula $V = ab^2/2$ as described previously (Harimoto et al., 2013). The mean tumour size ± SEM is shown. When the long axis of each tumour exceeded 20 mm, the mice were anaesthetized and sacrificed according to the NIH guidelines.

2.4. Administration of anti-PD-1 mAb to Hepa1-6-1 implanted B6 mice

The Hepa1-6-1 implanted mice were administered three distinct doses of an anti-PD-1 mAb (clone RMP1-14; BioXcell, NH) (100, 10, or 1 μg/mouse) 3 times i.p. at 5-day intervals on day 5, day 10 and day 15 after implantation of tumour cells.

2.5. Tumour-infiltrating lymphocyte (TIL) isolation

Excised tumours were cut into pieces, digested in RPMI 1640 medium containing 1 mg/ml Collagenase D (Merck, NJ) for 45 min at 37 °C and then crushed and filtered through a 77-μm nylon mesh (Flonchemical, Osaka, Japan). For isolation of TILs, cells collected from a mixed suspension of tumour cells and other haematopoietic cells were further separated using a Lympholyte-M gradient separation kit (Cedarlane, Burlington, ON, Canada).

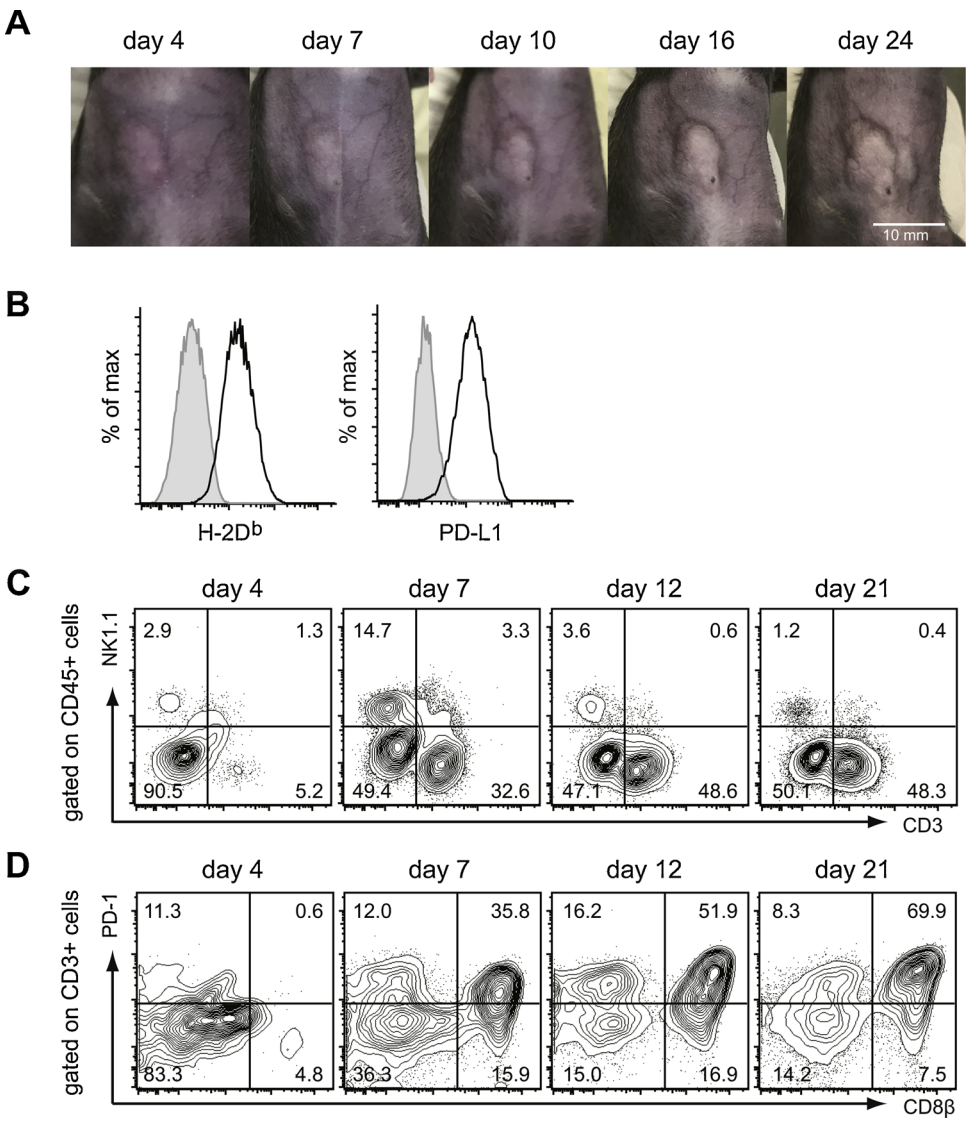

Fig. 1. Appearance of CD8β$^+$PD-1$^+$ CTLs within the Hepa1-6-1 tumour mass.
(A) Assessment of tumour growth in the untreated mice from day 4 to day 24 after Hepa1-6-1 cell s.c. implantation (scale bar, 10 mm). (B) The intensity of the class I MHC molecules (left) and PD-L1 expression (right) on Hepa1-6-1 cells (solid curve). (C) Flow cytometry analysis of the NK1.1$^+$ CD3$^+$ cells within the Hepa1-6-1 tumour mass on days 4, 7, 12, and 21 after implantation of Hepa1-6-1 cells (gated on CD45$^+$ cells). This experiment was performed three times under similar conditions, yielding similar results. (D) Flow cytometry analysis of CD8β$^+$ PD-1$^+$ cells within the Hepa1-6-1 tumour mass on days 4, 7, 12, and 21 after implantation of Hepa1-6-1 cells (gated on CD3$^+$ cells). This experiment was performed three times under similar conditions, yielding similar results.

2.6. Depletion of CD8β$^+$ T cells in vivo

Depletion of CD8β$^+$ T cells in B6 mice was achieved by i.p. injection of anti-mouse CD8β mAb (clone 53-5.8; BioXcell, NH) (100 μg/mouse) 2 days prior to tumour implantation and was followed by additional CD8β mAb injections after tumour implantation (on days 7 and 14). We confirmed that more than 95% of the CD8β + T cells had been depleted in the Spleen by flow cytometry.

2.7. Induction of bone marrow-derived DCs

Bone marrow-derived DCs were generated using bone marrow (BM) cells from the femurs and tibias of B6 mice. BM cells were depleted of red blood cells via osmotic haemolysis. A total of 1×10^6 BM cells was incubated in CCM containing 3.3 ng/ml murine recombinant GM-CSF (Peprotech, Rocky Hill, NJ) in 24-well tissue culture plates. On day 2 of culture, the floating cells were gently removed; then, 1×10^5 Hepa1-6-1 cells were added to the Transwell system in fresh medium (Corning, NY). On day 5, non-adherent cells were collected and used as bone marrow-derived DCs.

2.8. Purification of CD11c$^+$ DCs from TILs

A TIL suspension was prepared from collagenase-treated tumour mass, and then mouse CD11c$^+$ magnetic nanobeads were added to the suspension as manufacturer instructions (StemCell Technologies, BC, Canada). CD11c$^+$ cells were positively sorted using a magnetic separator. We confirmed that approximately 95% purified CD11c$^+$ cells were in collected cells.

2.9. Re-stimulation of Hepa1-6-primed lymphocytes with DCs

A total of 1×10^6 Hepa1-6 cells in 200 μl of PBS was implanted into each syngeneic B6 mouse via i.p. injection on days 0 and 14. On day 21, splenic CD8$^+$ T cells were obtained using a nylon wool column. A total of 5×10^5 splenic T cells were purified and labelled with 5 mM carboxyfluorescein diacetate succinimidyl ester (CFSE) (Merck) and then cultured with 1×10^5 DCs in 200 μl of CCM in a 96-well flat-bottomed tissue culture plate for 4 days. The re-stimulated cells were analysed by flow cytometry for cell proliferation assay.

2.10. CTL assay

Effector cells were incubated with 5×10^3 ^{51}Cr-labelled target cells for 4 h at 37 °C in 200 μl of RPMI 1640 medium containing 10% heat-inactivated FCS in 96-well U-bottomed tissue culture plates. The plates were centrifuged for 5 min at 200 × *g*, and 100 μl of each supernatant was harvested to determine the ^{51}Cr count by using a Wallac Wizard 3”

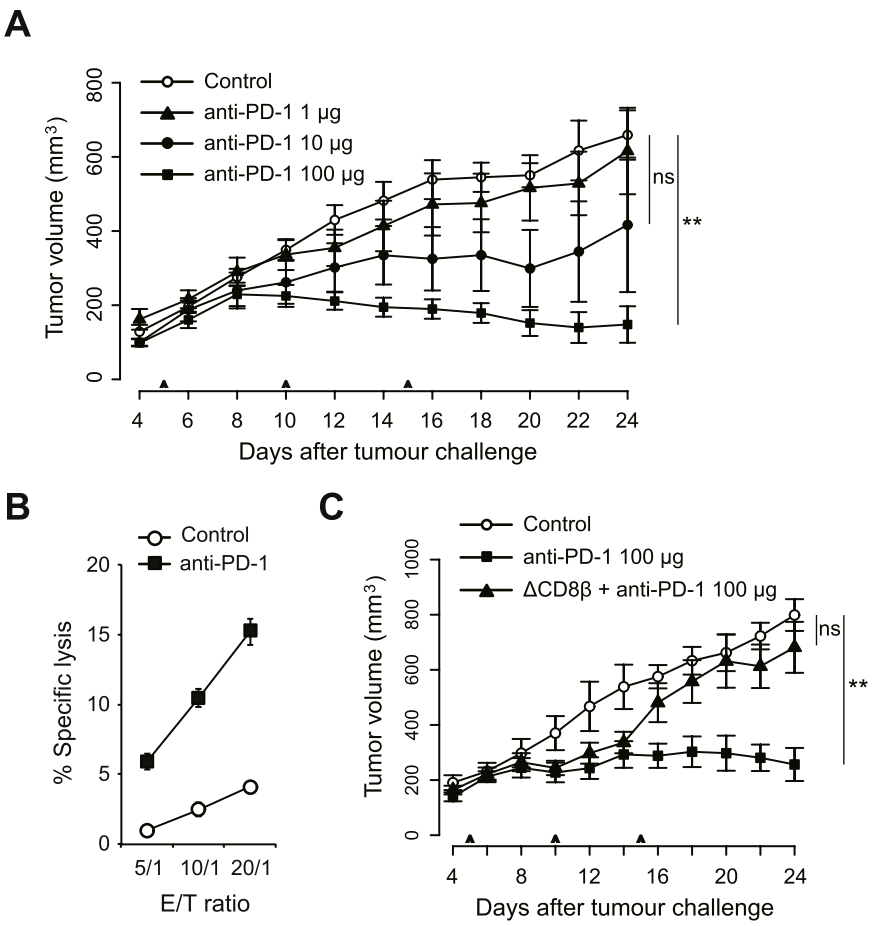

Fig. 2. Anti-tumour effect of the anti-PD-1 mAb on Hepa1-6-1 cells.
(A) Tumour growth curves of the Hepa1-6-1 cells in B6 mice treated with 100 μg of anti-PD-1 mAb (clone RMP1-14). The B6 mice were implanted with Hepa1-6-1 cells in the abdominal region. The anti-PD-1 mAb was administered three times via i.p. injection on day 5, day 10 and day 15 after implantation of the tumour cells (shown as "^" in the graph). The tumour mass volume was calculated using the formula $V = ab^2/2$ (V, the tumour volume; a, the major axis of the tumour; b, the minor axis of the tumour). The mean tumour size ± SEM is shown (n = 6 mice per group). The data were analysed using a Mann-Whitney U test; **: p-value < 0.01; ns: not significant. (B) To evaluate the effect of the anti-PD-1 mAb on TILs within the Hepa1-6-1 tumour mass, B6 mice were treated three times via i.p. injection with 100 μg of anti-PD-1 mAb on day 5, day 10 and day 15 after implantation of the tumour cells. Then, a standard ^{51}Cr release assay was performed on day 16 (n = 3 mice per group). (C) Tumour growth curves of the Hepa1-6-1 cells in B6 mice with deleted CD8$^+$ T cells. The anti-PD-1 mAb (100 μg/mouse) was administered three times i.p. on day 5, day 10 and day 15 after implantation of the tumour cells (shown as "^" in the graph). The tumour mass volume was calculated using the formula $V = ab^2/2$ (a, the major axis of the tumour; b, the minor axis of the tumour). The mean tumour size ± SEM is shown (n = 6 mice per group). The data were analysed using a Mann-Whitney U test; **: p-value < 0.01; ns: not significant.

1480 Gamma Counter (Perkin Elmer, MA). Maximum ^{51}Cr release was defined as the count obtained in the supernatant of 5×10^3 target cells, maintained in 100 μl of RPMI 1640 medium containing 10% heat-inactivated FCS, that were lysed with 100 μl of 2.5% Triton X-100 (FUJIFILM Wako Pure Chemical Corporation, Osaka, Japan). Spontaneous ^{51}Cr release was measured by the addition of 100 μl of RPMI 1640 medium containing 10% heat-inactivated FCS instead of Triton X-100. The corrected percent lysis for each effector cell concentration was calculated using the mean cpm for each replicate of wells, as follows: corrected % lysis = 100 × (experimental ^{51}Cr released – spontaneous release) / (maximum release – spontaneous release).

2.11. Flow cytometry analyses

Draining lymph nodes (DLNs) and spleens were harvested at the same time the tumours were excised. The DLNs and spleen were crushed and filtered through a 77-μm nylon mesh (Flonchemical). The tumours were treated using the same method described for tumour-infiltrating lymphocyte isolation. The TILs, DLNs or splenocytes were pre-incubated with anti-mouse CD16/CD32 (clone 93; BioLegend) for 10 min at 4 °C prior to membrane staining. The cells were stained with the relevant antibodies for 30 min at 4 °C in PBS with 2% heat-inactivated FCS and 0.1% sodium azide and washed twice. The anti-mouse antibodies CD3-FITC (145-2C11), CD3-PE (145-2C11), CD8β-APC (YTS156.7.7), CD44-PE-Cy7 (IM7), CD69-PE-Cy7 (H1.2F3), CD80-PE (16-10A1), CD103-APC-Cy7 (2E7), CD107a-PE (1D4B), CD161-BV421 (NK-1.1-BV421) (PK136), CD205-PE-Cy7 (DEC-205-PE-Cy7) (NLDC-145), CD279-PE (PD-1-PE) (J43), CD279-BV421 (PD-1-BV421) (29 F.1A12), Dendritic Cell Marker-APC (33D1), H-2D^b-FITC (KH95), and I-A/I-E-FITC (M5/114.15.2) were purchased from BioLegend (CA, USA). The anti-mouse antibodies CD11c-BV786 (HL3), CD45-BV510 (30-F11), CD86-BV421 (GL1), CD161-BUV395 (NK-1.1-BUV395) (PK136), CD273-BUV395 (PD-L2-BUV395) (TY25), CD274-BV711 (PD-L1-BV711) (MIH5), and CD279-PE (PD-1-PE) (J43) were purchased from BD Biosciences. The anti-mouse CD62L-FITC (MEL-14) antibody was purchased from Thermo Fisher Scientific. Dead cells were excluded by staining with propidium iodide. Stained samples were evaluated on a BD LSRFortessa X-20 18 colour cytometer (BD Biosciences), and the analyses were performed with FlowJo software (BD Biosciences).

2.12. Activation of tolerogenic DCs in vivo by i.p. injection of α-GalCer in Hepa1-6-1 implanted B6 mice and CD1d$^{-/-}$ mice

Mice were administered α-GalCer (2 μg/mouse) via i.p. injection every other day from day 0 to day 18 (for a total of 10 injections). α-GalCer was dissolved in 0.5% polyoxyethylene sorbitan monolaurate (FUJIFILM Wako Pure Chemical Corporation, Osaka, Japan) as the vehicle according to the manufacturer's instructions and diluted with PBS to a 20 μg/ml concentration.

2.13. Measurement of cytokines in the serum of Hepa1-6-1 implanted B6 mice

On day 16, sera were collected from B6 mice treated with α-GalCer or anti-PD-1 mAb and analysed by ELISA. The interleukin-12 (IL-12), interferon-gamma (IFN-γ) and tumour necrosis factor-alpha (TNF-α) levels were measured with an IL-12p40 detection kit (R&D Systems, Minneapolis, MN), IFN-γ detection kit, or TNF-α detection kit (BioLegend), respectively, according to the manufacturer's instructions.

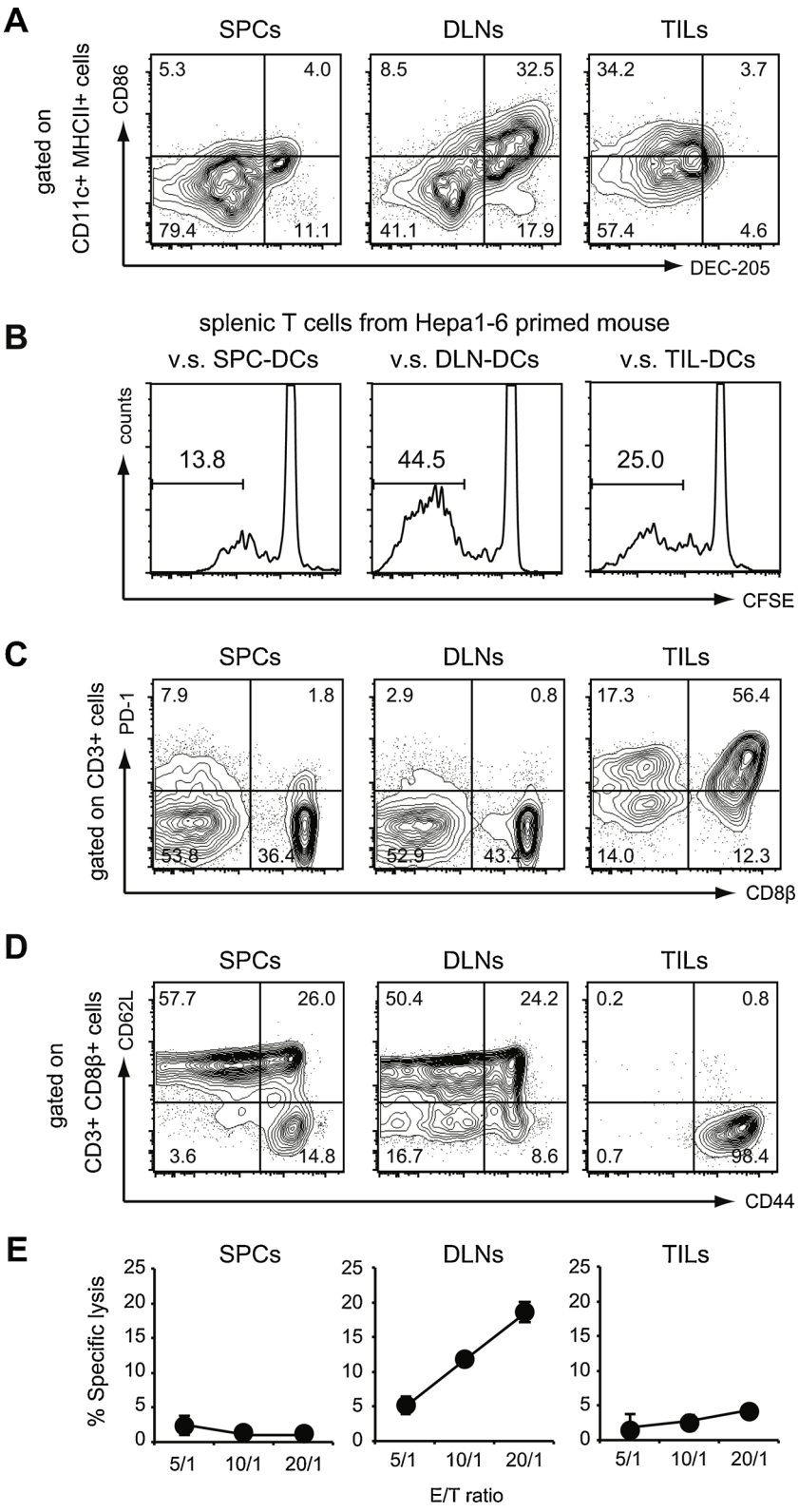

Fig. 3. Each state of DCs and CTLs in the spleen, DLNs or TILs. (A) Flow cytometry analysis of DCs in the spleen, DLNs or TILs on day 16 after implantation of Hepa1-6-1 cells in B6 mice (gated on $CD11c^+$ class II MHC^+ cells). (B) CFSE-labelled splenic T cells from Hepa1-6-primed B6 mice were stimulated for 4 days with DCs from the spleen (SPC-DCs, left panel), DLNs (DLN-DCs, middle panel) or TILs (TIL-DCs, right panel) of untreated B6 mice on day 16 after implantation of Hepa1-6-1 cells. After that, the harvested cells were analysed by flow cytometry for cell proliferation assay. (gated on $CD8\beta^+$ cells). (C, D) Flow cytometry analysis of DCs in the spleen, DLNs or TILs on day 16 after implantation of Hepa1-6-1 cells in B6 mice (gated on $CD3^+$ cells in Fig. 3C, and on $CD3^+$ $CD8\beta^+$ cells in Fig. 3D). (E) To evaluate the cytotoxicity of CTLs in the spleen, DLNs or TILs against Hepa1-6-1 cells, a standard ^{51}Cr release assay was performed on day 16 after implantation of Hepa1-6-1 cells in B6 mice ($n = 3$ mice per group). This experiment was performed three times under similar conditions, yielding similar results.

2.14. Statistical analysis

The data analysis was performed with R 3.5.1 software (R Foundation for Statistical Computing, Vienna, Austria; https://www.R-project.org/). Differences between treatment groups of interest were analysed using Student's *t*-test or a Mann-Whitney U test. All statistical results were considered significant at a p-value < 0.05.

3. Results

3.1. Appearance of $CD8\beta^+$ $PD\text{-}1^+$ CTLs within the growing Hepa1-6-1 tumour mass

We observed steady growth of Hepa1-6-1 cells from days 4 to 24 when B6 mice were implanted s.c. with syngeneic Hepa1-6-1 cells

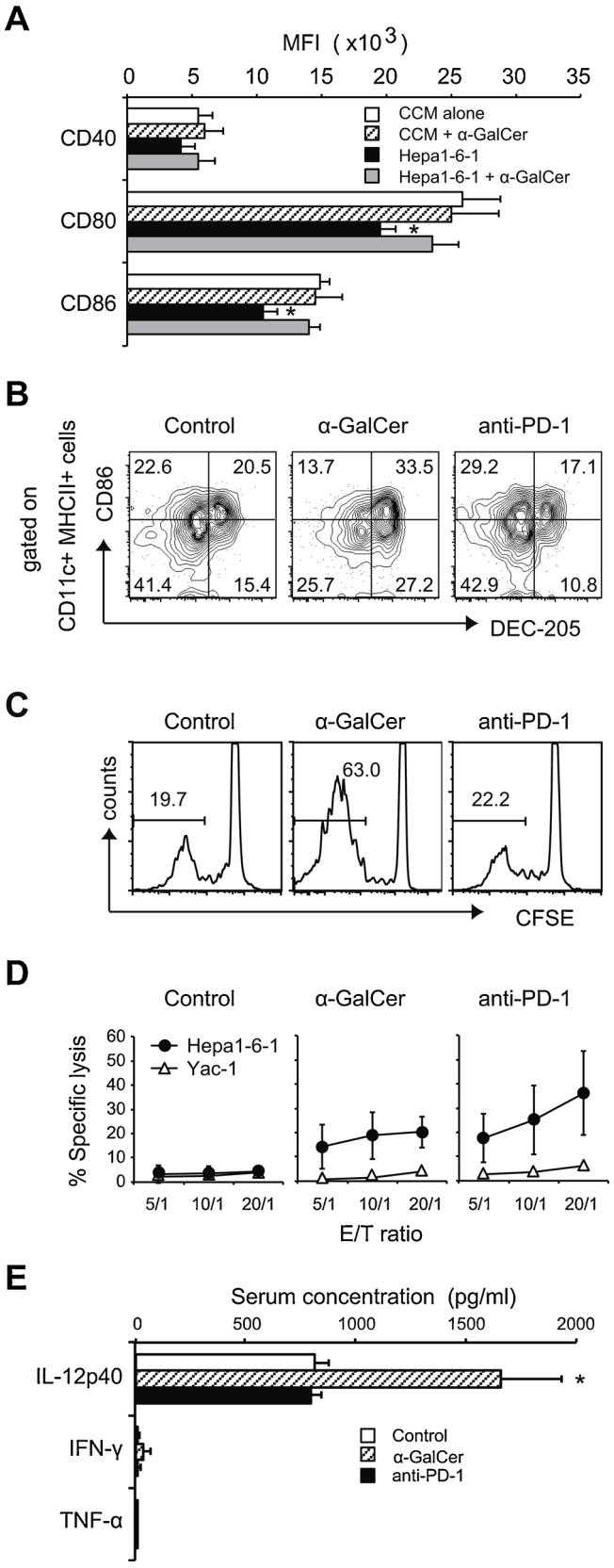

Fig. 4. Effect of anti-PD-1 mAb and α-GalCer administration on tolerogenic DCs.

(A) Flow cytometry analysis of CD40, CD80 and CD86 expression on bone marrow-derived DCs (gated on CD11c$^+$ class II MHC$^+$ cells). The bone marrow-derived DCs treated with or without 100 ng/ml α-GalCer were co-cultured with Hepa1-6-1 cells for 24 h. This experiment was performed three times under similar conditions, yielding similar results. The data were analysed using Student's *t*-test; *: p-value < 0.05. (B) Flow cytometry analysis of the DCs in TILs from B6 mice treated with anti-PD-1 mAb or α-GalCer on day 16 after implantation of Hepa1-6-1 cells. α-GalCer (2 μg/mouse) was administered to mice every other day from day 0 after implantation of Hepa1-6-1 cells for a total of 8 doses. Anti-PD-1 mAb (100 μg/mouse) was administered to mice three times, on day 5, day 10, and day 15 after implantation of Hepa1-6-1 cells (gated on CD11c$^+$ class II MHC$^+$ cells). (C) CFSE-labelled splenic T cells from Hepa1-6-primed mice were stimulated for 4 days with DCs in the TILs from α-GalCer-treated or anti-PD-1 mAb-treated mice on day 16 after Hepa1-6-1 cell implantation. α-GalCer (2 μg/mouse) was administered every other day from day 0 to day 14 after implantation of Hepa1-6-1 cells. Anti-PD-1 mAb (100 μg/mouse) was administered on day 5, day 10 and day 15 after implantation of Hepa1-6-1 cells. The co-cultured cells were harvested and analysed to determine the number of cell divisions using flow cytometry (gated on CD8β$^+$ cells). (D) To evaluate the ex vivo cytotoxicity of TILs in B6 mice treated with α-GalCer or anti-PD-1 mAb, a standard ^{51}Cr release assay was performed on day16 after Hepa1-6-1 cell implantation (n = 3 mice per group). α-GalCer (2 μg/mouse) was administered every other day from day 0 to day 14. Anti-PD-1 mAb (100 μg/mouse) was administered on day 5, day 10 and day 15. Hepa1-6-1 cells (closed circle) and Yac-1 cells (open triangle) were used as target cells. (E) The IL-12p40, IFN-γ, and TNF-α levels in the Hepa1-6-1-implanted B6 mouse sera were measured by ELISA on day 16 (n = 4 mice per group). Mice were treated with 2 μg/ml α-GalCer or 100 μg/ml anti-PD-1 mAb. α-GalCer was administered every other day from day 0 to day 14 after implantation of Hepa1-6-1 cells. Anti-PD-1 mAb was administered on day 5, day 10 and day 15 after implantation of Hepa1-6-1 cells. The data were analysed using Student's *t*-test; *: p-value < 0.05.

(Fig. 1A) that stably expressed D^d class I MHC molecules and PD-L1 (Fig. 1B). When we examined the CD45$^+$ leukocytes within the growing Hepa1-6-1 tumour mass on days 4, 7, 12, and 21, we confirmed that the number of NK1.1$^+$ NK cells reached a maximum on day 7 and decreased after implantation of the Hepa1-6-1 cells (Fig. 1C), and the number of PD-1$^+$ CD8β$^+$ Hepa1-6-1-specific CTLs increased after reduction of the NK1.1$^+$ NK cell population (Fig. 1D).

3.2. Effects of i.p. administration of anti-PD-1 check-point blockade on Hepa1-6-1 tumour growth

As expected, three i.p. injections of the anti-PD-1 check-point blockade dose-dependently inhibited the growth of the Hepa1-6-1 cell mass (Fig. 2A). Moreover, CTL cytotoxicity against Hepa1-6-1 cells was increased after treatment with 100 μg anti-PD-1 mAb (Fig. 2B). We also observed the effect of anti-PD-1 mAb on the mice with depleted CD8β$^+$ cells and confirmed that CD8β$^+$ cells within the Hepa1-6-1 tumour mass were tumour-specific CTLs (Fig. 2C).

3.3. Identification of the priming region within the Hepa1-6-1 cell-implanted mice

The above findings indicate that the temporarily increased NK cells may recognize the growing Hepa1-6-1 cells as foreign; then, the released Hepa1-6-1 fragments are captured and cross-presented via class I MHC molecules by neighbouring DCs to prime naïve T cells. If the primed T cells are specific PD-1$^+$ CD8β$^+$ CTLs, they may invade into the growing PD-L1$^+$ Hepa1-6-1 tumour mass to form PD-1/PD-L1 engagements. To confirm this possibility, we carefully examined the DCs throughout the Hepa1-6-1 tumour mass and found that the DEC-205$^+$ DCs within the TILs were tolerogenic and exhibited downregulated expression of the CD86 co-stimulatory molecule (right panel of Fig. 3A). Additionally, splenic DEC-205$^+$ DCs in the Hepa1-6-1 implanted mice were tolerogenic (left panel of Fig. 3A). In contrast, DEC-205$^+$ DCs in the draining lymph node (DLN-DCs) exhibited upregulated co-stimulatory molecule expression (middle panel of Fig. 3A). Thus, we stimulated Hepa1-6-primed spleen cells with these DCs and confirmed that

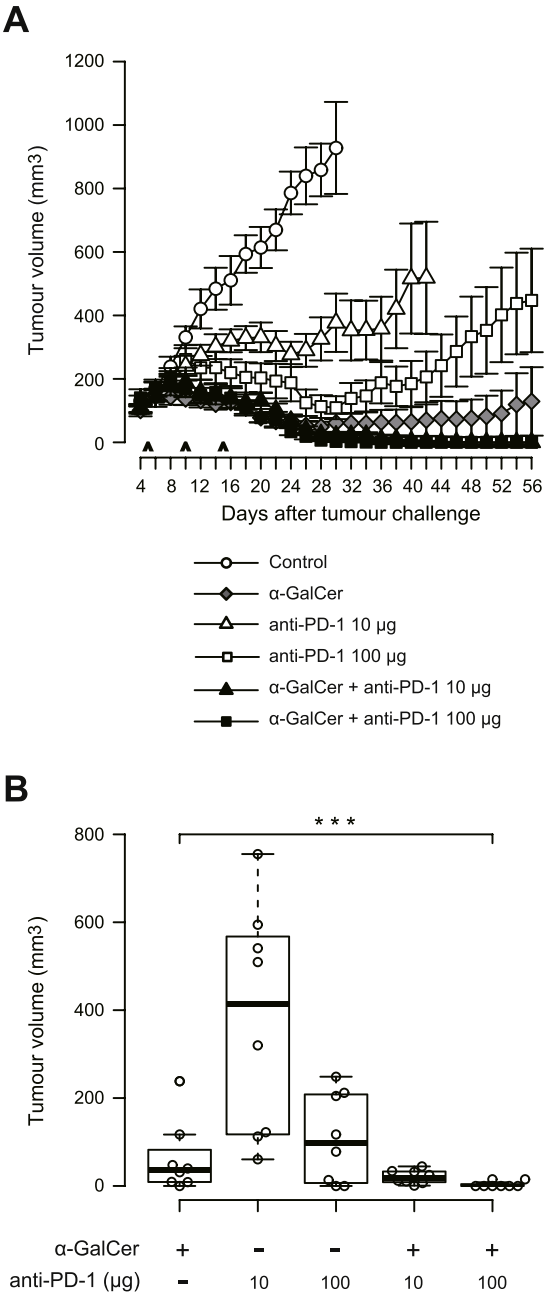

Fig. 5. Effect of combination therapy with anti-PD-1 mAb and α-GalCer on tumour growth.
(A) Tumour growth curves of Hepa1-6-1 cells in B6 mice treated with anti-PD-1 mAb with or without α-GalCer. Anti-PD-1 mAb (100 μg/mouse, 10 μg/mouse) was administered i.p. to mice three times, on day 5, day 10 and day 15 after implantation of Hepa1-6-1 cells (shown as "^" in the graph). α-GalCer (2 μg/mouse) was administered to mice i.p. ten times, every other day from day 0 to day 18. The tumour mass volume was calculated using the formula $V = ab^2/2$ (a, the major axis of the tumour; b, the minor axis of the tumour). The mean tumour size ± SEM is shown (n = 8 mice per group). (B) Boxplot showing tumour volume at day 30 after Hepa1-6-1 cell implantation, as described in Fig. 5A (n = 8 mice per group). The data were analysed using a Mann-Whitney U test; ***: p-value < 0.001.

the DLN-DCs showed a strong ability to stimulate primed spleen cells (Fig. 3B). Therefore, DLN-DCs within the Hepa1-6-1-implanted mice had the ability to specifically expand CD8β$^+$ CTLs from the primed T cells. Notably, the CD8β$^+$ CTLs observed within the Hepa1-6-1 mass (TILs) became PD-1$^+$ CD8β$^+$ CTLs, although they were originally PD-1$^-$ cells (Fig. 3C); conversely, the CTLs observed within the DLN were PD-1$^-$ CD62$^+$ CD44$^+$ central memory T cells (Fig. 3D), suggesting that CD8β$^+$ CTLs within the tumour mass gained PD-1 expression. Taken together, our results show that tumour-specific CD8β$^+$ CTLs are established within draining lymph nodes (DLNs) through immunogenic DCs if they are unaffected by tumour-derived factors (Yu, et al., 2012). Moreover, CD8β$^+$ CTLs induced within DLNs become tumour-specific PD-1- CD8β$^+$ CTLs and invade into growing tumours, where they gain PD-1$^+$ expression within the tumour mass. Then, strong engagement between PD-1 on CD8β$^+$ CTLs and PD-L1 on Hepa1-6-1 cells is established within the tumour mass. As demonstrated here, CTL cytotoxicity against Hepa1-6-1 cells was detected within the DLNs; in contrast, the TILs or SPCs within the Hepa1-6-1-bearing mice did not show specific CTL cytotoxicity against Hepa1-6-1 cells (Fig. 3E).

3.4. Tolerogenic DCs with down-modulated co-stimulation molecule expression became immunogenic DCs with upregulated expression of co-stimulation molecules by repetitive stimulation with α-GalCer

DCs incubated with Hepa1-6-1-derived factors for 2 days became tolerogenic with down-modulated co-stimulatory molecule (CD40, CD80 and CD86) expression (Fig. 4A). As recently demonstrated (Ichikawa et al., 2016; Kogo et al., 2017; Murakami et al., 2015; Otsuka et al., 2018), after a 24-h incubation of tolerogenic DCs with 100 ng/ml α-GalCer, an immuno-potent lipid/glycolipid that converts tolerogenic DCs into an immunogenic state, the treated DCs became activated and exhibited enhanced expression of co-stimulatory molecules (Fig. 4A and B) that specifically stimulated Hepa1-6-primed splenic T to proliferate (Fig. 4C). Moreover, after i.p. injection of 2 μg/mouse of α-GalCer every other day, functional CD8$^+$ PD-1$^+$ CTLs were observed within the Hepa1-6-1 tumour mass (Fig. 4D). Furthermore, the α-GalCer-activated DCs secreted a large amount of IL-12, which can activate tumour-specific CTLs in vivo (Fig. 4E).

3.5. Effect of i.p. administration of anti-PD-1 mAb and α-GalCer on Hepa1-6-1 tumour growth

We next examined the effect of check-point blockade on co-stimulatory molecule expression in tolerogenic DCs in vivo. During our entire investigation, enhancement of co-stimulatory molecule expression was not observed within the Hepa1-6-1 tumour mass when the mice were administered three i.p. injections of anti-PD-1 mAb (Fig. 4B). Thus, we investigated the effect of termination of the check-point blockade on Hepa1-6-1 cell growth in our mouse model.

As demonstrated in Fig. 5A, although administration of either 10 μg/mouse (open triangle) or 100 μg/mouse (open square) of the anti-PD-1 mAb three times resulted in partial and temporal growth inhibition of the implanted Hepa1-6-1 cells, Hepa1-6-1 tumour growth recurred even after the growth rate declined, indicating that the effect of the check-point blockade was not long-lasting; therefore, additional strategies were considered. On the basis of our recent findings showing that when mice were sequentially stimulated with i.p. α-GalCer every 48 h (for ten doses in total), tolerogenic DCs were converted to immunogenic DCs (Kogo et al., 2017), we tested the effect of α-GalCer as an additional stimulator along with the check-point blockade. We found that sequential administration with α-GalCer seemed to enhance the effect of the check-point blockade, and the amount of the check-point blockade needed for long-lasting inhibition was reduced by 90% (Fig. 5B).

3.6. Effect of α-GalCer i.p administration on tumour growth in CD1d$^{-/-}$ mice

Although we examined carefully in the kinetics of NK cell number and NKT cells by using flowcytometry, but we could not detect any differences among their numbers and cytotoxities when B6 mice were injected with α-GalCer showed apparent suppressive effect on Hepa1-6-

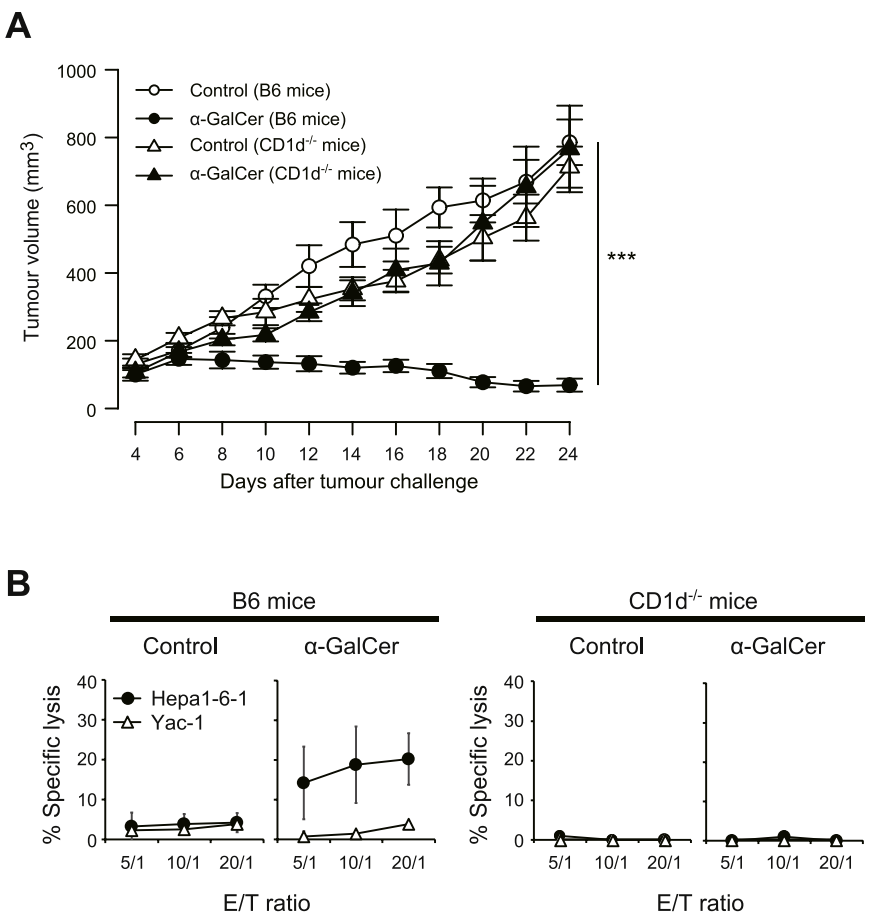

Fig. 6. Effect of α-GalCer i.p administration on tumour growth in CD1d$^{-/-}$ mice.
Although we examined carefully in the kinetics of NK cell number and NKT cells by using flowcytometry, but we could not detect any differences among them. Also, (A) Tumour growth curves of Hepa1-6-1 cells in B6 mice (n = 8 mice per group) and CD1d$^{-/-}$ mice on a B6 background (n = 6 mice per group). α-GalCer (2 μg/mouse) was administered to mice i.p. ten times, every other day from day 0 to day 18 after implantation of Hepa1-6-1 cells. The tumour mass volume was calculated using the formula $V = ab^2/2$ (a, the major axis of the tumour; b, the minor axis of the tumour). The mean tumour size ± SEM is shown. The data were analysed using a Mann-Whitney U test; ***: p-value < 0.001. (B) To compare the in vitro cytotoxicity of TILs obtained from B6 mice and CD1d$^{-/-}$ mice treated with α-GalCer, a standard ^{51}Cr-release assay was performed on day16 after the Hepa1-6-1 cell implantation (n = 3 mice per group). α-GalCer (2 μg/mouse) was administered every other day from day 0 to day 14. Hepa1-6-1 cells (closed circle) and Yac-1 cells (open triangle) were used as target cells.

1-spcific growing indicating that CD1d-related activated immunity may induce Hepa1-6-1-spcific suppression. Thus, we performed the experiments using CD1d$^{-/-}$ mice of B6 origin and confirmed that the mice will not induce Hepa1-6-1-spcific CTLs when administered with α-GalCer (Fig. 6A). Moreover, we could not detect any Hepa1-6-1-spcific CTLs and NKT cells at all when administered CD1d$^{-/-}$ mice of B6 origin with α-GalCer (left panel of Fig. 6B) although Hepa1-6-1-spcific CTLs were seen in the original B6 mice (right panel of Fig. 6B). Also, as we have reported recently (Tomita et al., 2019), CD1-restricted stimulation may correlate tumour-specific cytotoxicities.

4. Discussion

As we demonstrated here, when 100 μg of anti-PD-1 mAb was inoculated three times into mice with growing Hepa1-6-1 cells, the Hepa1-6-1 cell expansion was stopped, and a reduction in growth was observed. This reduction may be a result of breaking of the mutual engagement by the anti-PD-1 treatment and release of the tethered PD-1$^+$ CTLs, allowing them to be functional. Here, we confirmed the presence of increased NK cells in the early stages of tumour growth. The NK cells within the tumour mass may kill Hepa1-6-1 cells, and the released Hepa1-6-1 fragments are captured and cross-presented via class I MHC molecules by the neighbouring DEC-205$^+$ DCs (Bozzacco et al., 2007) to prime naïve T cells (Hsu et al., 2018). If the primed T cells become specific CD8β$^+$ PD-1$^+$ CTLs, they may invade into the Hepa1-6-1 tumour mass to form PD-1/PD-L1 engagements (Kumari et al., 2013).

We carefully examined DCs throughout the Hepa1-6-1 tumour mass and confirmed that the DEC-205$^+$ DCs within the TILs were tolerogenic and exhibited downregulated co-stimulatory molecule expression. The splenic DEC-205$^+$ DCs in the Hepa1-6-1-implanted mice were also tolerogenic. In contrast, DEC-205$^+$ DCs in the draining lymph nodes (DLN-DCs) exhibited upregulated co-stimulatory molecule expression and were immunogenic (Yu et al., 2012). Thus, we speculate that naïve T cells might be primed by the immunogenic DEC-205$^+$ DCs that capture NK cell-released fragmented tumour antigen(s) in the body; then, the primed naïve T cells may become activated Hepa1-6-1-specific CD8$^+$ CTLs in vivo. Strong engagement between PD-1 on the CD8β$^+$ CTLs and PD-L1 on the Hepa1-6-1 cells was established within the tumour mass. Thus, CTL cytotoxicity against Hepa1-6-1 cells was induced within the DLNs, and TILs or SPCs within the Hepa1-6-1-implanted mice did not show any specific CTL cytotoxicity when a check-point blockade was administered.

Taken together, our results show that tolerogenic DCs were dominant within the tumour mass and that DCs in the tumours remained tolerogenic to prevent the induction of tumour-specific CD8β$^+$ CTLs even after several check-point blockade treatments. After three i.p. injections of anti-PD-1 mAb, we stopped administration of the anti-PD-1 mAb and investigated tumour growth. Although the growth of the Hepa1-6-1 tumour temporarily declined, growth recurred over time, indicating that the effect of the check-point blockade was not long-lasting under the control of tolerogenic DCs. Therefore, another alternative strategy was considered to convert tolerogenic DCs into immunogenic DCs, which may help to initiate specific immunity.

As shown here, enhancement of co-stimulatory molecule expression was not observed following check-point blockade treatment. However, stimulation of CD1d molecules on DCs with a specific lipid ligand, such as α-GalCer (Ichikawa et al., 2016; Murakami et al., 2015; Otsuka et al., 2018), altered the expression of co-stimulatory molecules (CD80, CD86, and CD40) on the tolerogenic DCs, and the DCs converted to an immunogenic state and secreted a large amount of IL-12, which can activate tumour-specific CTLs in vivo. Additionally, when mice were stimulated with α-GalCer to convert tolerogenic DCs into immunogenic DCs, the effect of PD-1 mAb seemed to be far stronger than expected,

and complete inhibition was observed when the mice were sequentially injected i.p. with 2 μg of α-GalCer together with either 10 μg/mouse or 100 μg/mouse of the anti-PD-1 mAb. Indeed, the effect of the check-point blockade was markedly enhanced when tolerogenic DCs were transformed into immunogenic DCs by stimulation with their CD1d ligand, thus reducing the required anti-PD-1 mAb dose by 90%. These results indicate that in some tumours, it might be better to activate tolerogenic DCs within the tumour mass by using lipids, such as α-GalCer, that will bind CD1d molecules on DCs because inducing this conversion to immunogenic DCs suppresses tumour growth better than check-point blockade alone. Although the magnitude was much weaker, as shown in the supplemental Fig. S1 (A, B), similar synergistic suppressive results are observed when B16F10 cells were applied to this system.

Fig. S1 Effect of combination therapy with anti-PD-1 mAb and α-GalCer on growth of B16F10 melanoma tumour mass.

(A) Tumour growth curves of B16F10 cells in B6 mice treated with anti-PD-1 mAb with or without α-GalCer. Anti-PD-1 mAb (100 μg/mouse) was administered i.p. to mice three times, on day 5, day 10 and day 15 after implantation with 1×10^5 B16F10 cells in the abdominal region subcutaneously (shown as "^" in the graph). α-GalCer (2 μg/mouse) was administered to mice i.p. ten times, every other day from day 0 to day 18. The tumour mass volume was calculated using the formula $V = ab^2/2$ (a, the major axis of the tumour; b, the minor axis of the tumour). The mean tumour size ± SEM is shown ($n = 4$ mice per group). When the long axis of each tumour exceeded 20 mm, the mice were anaesthetized and sacrificed according to the NIH guidelines. (B) Boxplot showing tumour volume at day 20 after B16F10 cell implantation, as described in Fig. S1A ($n = 4$ mice per group). The data were analysed using a Mann-Whitney U test; *: p-value < 0.05; ns: not significant.

Funding

This study was supported in part by grants from the Ministry of Education, Science, Sport, and Culture, the Ministry of Health and Labor and Welfare, Japan (25461715 and 16K09262 to H.T.); the Japanese Health Sciences Foundation; the Promotion and Mutual Aid Corporation for Private Schools of Japan; and from a MEXT-supported Program for the Strategic Research Foundation at Private Universities, Japan.

Declaration of Competing Interest

None.

Appendix A. Supplementary data

Supplementary material related to this article can be found, in the online version, at doi:https://doi.org/10.1016/j.imbio.2019.10.009.

References

Benson, D.M., Bakan, C.E., Mishra, A., Hofmeister, C.C., Efebera, Y., Becknell, B., Baiocchi, R.A., Zhang, J., Yu, J., Smith, M.K., Greenfield, C.N., Porcu, P., Devine, S.M., Rotem-Yehudar, R., Lozanski, G., Byrd, J.C., Caligiuri, M.A., 2010. The PD-1/PD-L1 axis modulates the natural killer cell versus multiple myeloma effect: a therapeutic target for CT-011, a novel monoclonal anti-PD-1 antibody. Blood 116, 2286–2294.

Blank, C., Gajewski, T.F., Mackensen, A., 2005. Interaction of PD-L1 on tumor cells with PD-1 on tumor-specific T cells as a mechanism of immune evasion: implications for tumor immunotherapy. Cancer Immunol. Immunother. 54, 307–314.

Bozzacco, L., Trumpfheller, C., Siegal, F.P., Mehandru, S., Markowitz, M., Carrington, M., Nussenzweig, M.C., Piperno, A.G., Steinman, R.M., 2007. DEC-205 receptor on dendritic cells mediates presentation of HIV gag protein to CD8+ T cells in a spectrum of human MHC I haplotypes. Proc. Natl. Acad. Sci. U. S. A. 104, 1289–1294.

Harimoto, H., Shimizu, M., Nakagawa, Y., Nakatsuka, K., Wakabayashi, A., Sakamoto, C., Takahashi, H., 2013. Inactivation of tumor-specific CD8(+) CTLs by tumor-infiltrating tolerogenic dendritic cells. Immunol. Cell Biol. 91, 545–555.

Hsu, J., Hodgins, J.J., Marathe, M., Nicolai, C.J., Bourgeois-Daigneault, M.C., Trevino, T.N., Azimi, C.S., Scheer, A.K., Randolph, H.E., Thompson, T.W., Zhang, L., Iannello, A., Mathur, N., Jardine, K.E., Kirn, G.A., Bell, J.C., McBurney, M.W., Raulet, D.H., Ardolino, M., 2018. Contribution of NK cells to immunotherapy mediated by PD-1/PD-L1 blockade. J. Clin. Invest. 128, 4654–4668.

Ichikawa, T., Negishi, Y., Shimizu, M., Takeshita, T., Takahashi, H., 2016. Alpha-galactosylceramide-activated murine NK1.1(+) invariant-NKT cells in the myometrium induce miscarriages in mice. Eur. J. Immunol. 46, 1867–1877.

Ishii, R., Shimizu, M., Nakagawa, Y., Shimizu, K., Tanaka, S., Takahashi, H., 2004. *In vivo* priming of natural killer T cells by dendritic cells pulsed with hepatoma-derived acid-eluted substances. Cancer Immunol. Immunother. 53, 383–390.

Kogo, H., Shimizu, M., Negishi, Y., Uchida, E., Takahashi, H., 2017. Suppression of murine tumour growth through CD8(+) cytotoxic T lymphocytes via activated DEC-205(+) dendritic cells by sequential administration of alpha-galactosylceramide in vivo. Immunology 151, 324–339.

Kozako, T., Yoshimitsu, M., Akimoto, M., White, Y., Matsushita, K., Soeda, S., Shimeno, H., Kubota, R., Izumo, S., Arima, N., 2011. Programmed death-1 (PD-1)/PD-1 ligand pathway-mediated immune responses against human T-lymphotropic virus type 1 (HTLV-1) in HTLV-1-associated myelopathy/tropical spastic paraparesis and carriers with autoimmune disorders. Hum. Immunol. 72, 1001–1006.

Kumari, A., Cacan, E., Greer, S.F., Garnett-Benson, C., 2013. Turning T cells on: epigenetically enhanced expression of effector T-cell costimulatory molecules on irradiated human tumor cells. J. Immunother. Cancer 1, 17.

Matsuhashi, T., Shimizu, M., Negishi, Y., Takeshita, T., Takahashi, H., 2014. A low, non-toxic dose of paclitaxel can prevent dendritic cell-precursors from becoming tolerogenic dendritic cells with impaired functions. Biomed. Res. 35, 369–380.

McDonnell, A.M., Prosser, A.C., van Bruggen, I., Robinson, B.W., Currie, A.J., 2010. CD8alpha+ DC are not the sole subset cross-presenting cell-associated tumor antigens from a solid tumor. Eur. J. Immunol. 40, 1617–1627.

Murakami, R., Nakagawa, Y., Shimizu, M., Wakabayashi, A., Negishi, Y., Hiroi, T., Okubo, K., Takahashi, H., 2015. Effects of dendritic cell subset manipulation on airway allergy in a mouse model. Int. Arch. Allergy Immunol. 168, 219–232.

Nakatsuka, K., Sugiyama, H., Nakagawa, Y., Takahashi, H., 1999. Purification of antigenic peptide from murine hepatoma cells recognized by class-I major histocompatibility complex molecule-restricted cytotoxic T-lymphocytes induced with B7-1-gene-transfected hepatoma cells. J. Hepatol. 30, 1119–1129.

Nizzoli, G., Larghi, P., Paroni, M., Crosti, M.C., Moro, M., Neddermann, P., Caprioli, F., Pagani, M., De Francesco, R., Abrignani, S., Geginat, J., 2016. IL-10 promotes homeostatic proliferation of human CD8(+) memory T cells and, when produced by CD1c(+) DCs, shapes naive CD8(+) T-cell priming. Eur. J. Immunol. 46, 1622–1632.

Otsuka, Y., Watanabe, E., Shinya, E., Okura, S., Saeki, H., Geijtenbeek, T.B.H., Takahashi, H., 2018. Differentiation of langerhans cells from monocytes and their specific function in inducing IL-22-specific Th cells. J. Immunol. 201, 3006–3016.

Prosser, M.E., Brown, C.E., Shami, A.F., Forman, S.J., Jensen, M.C., 2012. Tumor PD-L1 co-stimulates primary human CD8(+) cytotoxic T cells modified to express a PD1:CD28 chimeric receptor. Mol. Immunol. 51, 263–272.

Takahashi, H., Nakagawa, Y., Leggatt, G.R., Ishida, Y., Saito, T., Yokomuro, K., Berzofsky, J.A., 1996. Inactivation of human immunodeficiency virus (HIV)-1 envelope-specific CD8+ cytotoxic T lymphocytes by free antigenic peptide: a self-veto mechanism? J. Exp. Med. 183, 879–889.

Tomita, Y., Watanabe, E., Shimizu, M., Negishi, Y., Kondo, Y., Takahashi, H., 2019. Induction of tumor-specific CD8(+) cytotoxic T lymphocytes from naive human T cells by using Mycobacterium-derived mycolic acid and lipoarabinomannan-stimulated dendritic cells. Cancer Immunol. Immunother. 68 (10), 1605–1619. https://doi.org/10.1007/s00262-019-02396-8.

Yu, B., Ueta, H., Kitazawa, Y., Tanaka, T., Adachi, K., Kimura, H., Morita, M., Sawanobori, Y., Qian, H.X., Kodama, T., Matsuno, K., 2012. Two immunogenic passenger dendritic cell subsets in the rat liver have distinct trafficking patterns and radiosensitivities. Hepatology 56, 1532–1545.